

Complexation Enhanced Excited-State Deactivation by Lithium Ion Coordination to a Borondipyrromethene (Bodipy) Donor–Bridge–Acceptor Dyad

Andrew C. Benniston,^{*[a]} Songjie Yang,^[a] Helge Lemmetyinen,^[b] and Nikolai V. Tkachenko^{*[b]}

Keywords: Electron transfer / Charge transfer / Redox reactions / Coordination modes / Lithium

A donor–acceptor dyad was prepared comprised of a borondipyrromethene (Bodipy) chromophore as the acceptor and a dimethylamino moiety as the donor. The two groups are separated by a 2,2'-biphenol moiety. The excited state of the Bodipy is efficiently quenched by electron transfer involving donation from the dimethyl amino group. The rate constant for forward electron transfer in DMF was measured to be ca. $2 \times 10^{10} \text{ s}^{-1}$. The charge recombination process is ultra-

fast. Titration of aliquots of LiClO_4 to a DMF solution of the dyad resulted in alterations to the absorption spectrum associated with the 2,2'-biphenol unit. Changes were modelled as Li^+ ions bound to the oxygen atoms of the 2,2'-biphenol to produce 1:1 (Li^+ /ligand) and 2:1 (Li^+ /ligand) complexes. The rate constant for excited state quenching is enhanced upon lithium ion binding.

Introduction

Natural systems are proficient at manipulating the rates and pathways of electron transfer events by inducing or undergoing subtle structural effects.^[1] The protein environment in enzymes is often disposed to stabilising redox intermediates along what can often appear to be complicated or even near identical redox factors.^[2] The asymmetry in electron transfer in the photosynthetic reaction centre complex for the purple bacteria *Rhodospseudomonas viridis* is a prime example where redundancy in cofactors has evolved for the possible practical application of self-repair.^[3] The long-range migration of charge between cofactors within proteins further exemplifies how the subtleties within a multifaceted structure can be important.^[4] As complexity increases, as seen in neural networks, the control of electrical information transfer becomes crucial and more complex to comprehend.^[5] There are, of course, many lessons already learned from Nature, such as the need to couple proton movement with electron transfer,^[6] to protect high-energy intermediates^[7] and to divert destructive radical species

from sensitive areas of molecules.^[8] Many of these facets are the inspiration behind the construction and study of artificial mimicry systems.^[9] The supramolecular control of electron transfer within molecular architectures is an area of intense study.^[10] One aspect of such research has focused on the role of the bridge at mediating electron exchange, and identification of methods to control through-bond electronic coupling.^[11] Especially pertinent is the so called “angle effect” focusing primarily on the biphenyl unit and which seeks to correlate how factors such as triplet energy transfer,^[12] hole transport^[13] and electron transfer^[14] are modulated by dihedral angle conformation changes. Another highly topical field of study involves the effect of cation or anion chelation on electron transfer by their interaction with supramolecular structures. In particular, this endeavor seeks to achieve and document the stabilisation of photo-initiated redox states by cation/anion binding.^[15] In principle, these two facets may be combined into a single system where binding switches the angle and additionally perturbs the electronics. It is conceivable that both alterations can act in unison, completely counteract each other, or that one of the two factors has a dominant effect. Our interest was to identify a suitable molecular system to study these two effects. In particular, there was interest in seeing if some manner of “gate effect” might operate to discriminate between forward and return electron transfer. The first attempt at such a study uses the Bodipy-based dyad, **BD**, (Figure 1) which represents a simplified model where the dimethylamino quencher is separated from the photoactive group by a 2,2'-biphenol bridging unit. Two especially pertinent dihedral angles are ϕ and θ , which define the orienta-

[a] Molecular Photonics Laboratory, School of Chemistry, Newcastle University, Newcastle upon Tyne, NE3 1SQ, UK
E-mail: a.c.benniston@ncl.ac.uk
<http://www.ncl.ac.uk/mpl/>

[b] Department of Chemistry and Engineering, Tampere University, Tampere, Finland
E-mail: nikolai-.tkachenko@tut.fi
www.tut.fi/departments/chemistry-and-bioengineering/research/spc-group/index.htm

Supporting information for this article is available on the WWW under <http://dx.doi.org/10.1002/ejoc.201300867>.

tion of the two phenol rings. The former is expected to be close to 90° because of steric constraints imposed by the two methyl groups. The final angle essentially defines the twist between the two phenol rings and it is expected to control orbital overlap along the π -way.^[16] Cation chelation to the two alcohol groups was anticipated to both switch the conformation and perturb the orbital energies of the bridge. For this the lithium ion was chosen on the grounds that it prefers binding to hard oxygen centres,^[17] and its small size would polarize the O–H bond thus facilitating deprotonation. The dominant feature of the lithium binding appears to be electronic, and the alteration of redox potentials for the dyad.

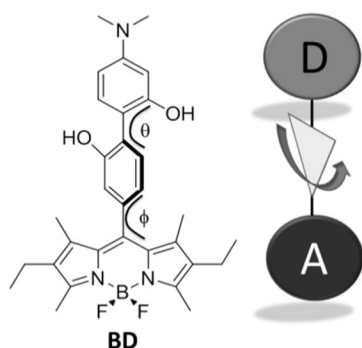


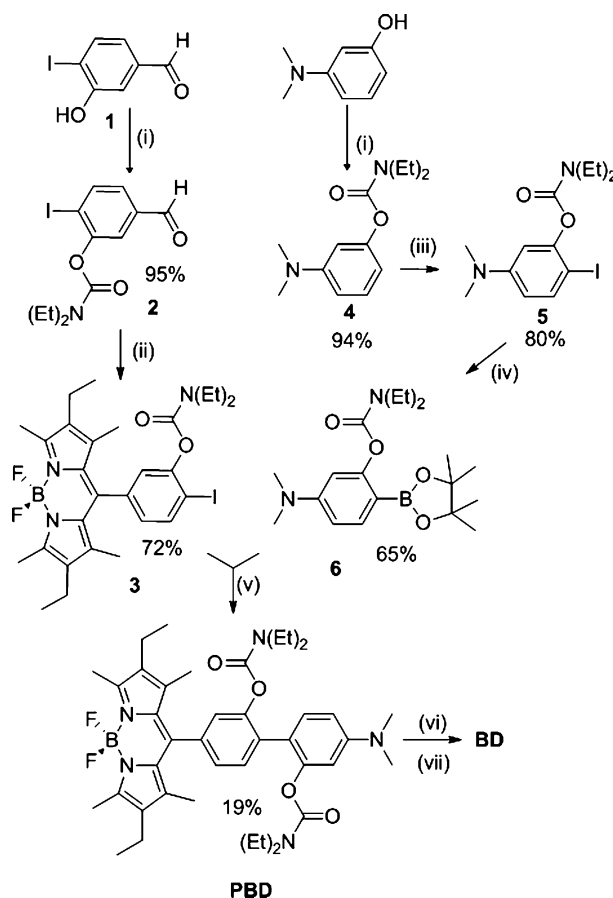
Figure 1. Representation of the donor–acceptor Bodipy dyad **BD** (left) and a simple cartoon showing how the central linker behaves as a gate-like moiety to manipulate electronic coupling (right).

Results and Discussion

Synthesis

Several different synthetic strategies were devised to prepare target molecule, **BD**. Scheme 1 represents the most successful approach to construction, and depends on formation of the 2,2'-biphenol unit as the penultimate step. The convergent synthesis required preparation of the two halves of the system. Compound **1** was prepared from 3-hydroxybenzaldehyde using a literature reported procedure.^[18] The hydroxyl moiety was protected as diethylcarbamate **2** in excellent yield. The next step involved building into place the Bodipy group using the standard procedures of reacting **2** with 3-ethyl-2,4-dimethylpyrrole, oxidation and finally chelation to the BF₂ unit.^[19] The identity of red solid **3**, prepared in 72% yield, was confirmed principally by ¹H, ¹⁹F and ¹¹B NMR spectroscopy. The second half of the compound was prepared starting from 3-(dimethylamino)phenol, which was again protected as *N,N*-diethylcarbamate **4**. Regioselective iodination of **4** produced **5** and analytical data were in agreement with previously reported data sets.^[20] Introduction of the boronic group to protected phenol **5** worked well using pinacolborane and palladium catalyst to afford **6**. Coupling of **3** and **6** under standard Suzuki coupling conditions afforded protected Bodipy **PBD** as a red solid in 19% yield. The deprotection of **PBD** is interesting since conditions had to be controlled carefully.

Initial efforts using NaOH in methanol afforded the mono-protected product which was isolated, and the final protecting group was removed using KOH in an ethanol/water mixture. Revision of this overall procedure in which the latter conditions were exclusively applied led to products that were difficult to purify. Though difficult to purify, product **BD** was ultimately identified by standard analytical methods. Full assignment of the ¹H NMR spectrum (see Supporting Information) was carried out by COSY.



Scheme 1. Reagents and conditions: (i) Et₂NCOCI, Et₃N, pyridine, THF, reflux; (ii) 3-ethyl-2,4-dimethylpyrrole, TFA, DCM, DDQ, (iPr)₂EtN, BF₃·Et₂O; (iii) *s*BuLi, TMEDA, iodine, THF; (iv) pinacolborane, triethylamine, PdCl₂(PPh₃)₂, THF; (v) DME, Na₂CO₃, Pd(PPh₃)₄; (vi) NaOH, MeOH; (vii) KOH, EtOH/H₂O.

Absorption & Fluorescence

The electronic absorption spectrum for **BD** in dry DMF is illustrated in Figure 2. The typical narrow Bodipy-based S₀–S₁ electronic absorption is located at $\lambda_{\text{ABS}} = 520$ nm. A slightly structured absorption is seen below 400 nm with a peak maximum at 320 nm. The overall profile can be identified as a superimposition of the Bodipy-based S₀–S₂ absorption profile and slightly redshifted electronic ¹A–¹L_a and ¹A–¹L_b π – π^* transitions for the 2,2'-biphenol group. Extremely weak fluorescence is observed from a dilute DMF solution of the dyad at a peak maximum $\lambda_{\text{EM}} = 542$ nm. The emission profile is a reasonable mirror image

of the sharp long-wavelength Bodipy-based absorption profile. The measured quantum yield of fluorescence (ϕ_{FLU}) is 0.01, which is reduced significantly when compared to basic 8-phenyl-Bodipy ($\phi_{\text{FLU}} = 0.69$).^[21] Excited-state deactivation of the first-excited singlet state for **BD** is extremely efficient. It is noticeable that the fully-corrected excitation spectrum for the high-energy region does not match with the absorption spectrum (Figure 2, inset). Not all photons collected at the 2,2'-biphenol site migrate to the Bodipy group. It would appear that the efficiency of energy transfer across the bridge to the Bodipy is low.

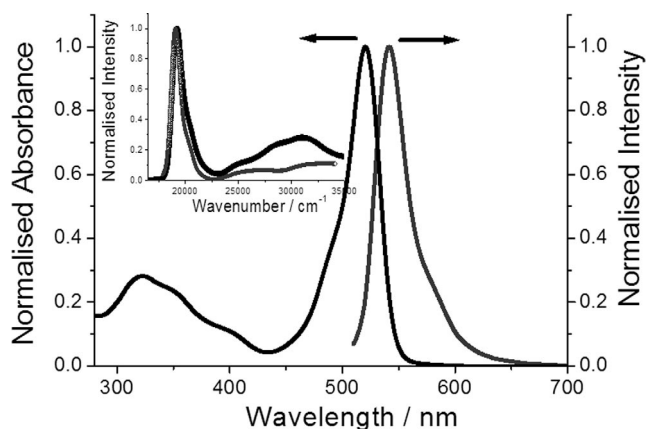


Figure 2. Absorption (black) and emission (grey) spectra for **BD** in dry DMF. Inset shows a comparison of the absorption spectrum (black) and the fully-corrected fluorescence excitation spectrum (grey).

Clear identification of the dimethylamino site as the source for excited-state quenching was confirmed by fluorescence spectroscopy and a simple acid titration. Thus, addition of trifluoroacetic acid to a solution of **BD** in MeCN resulted in ≈ 20 -fold increase in emission at 542 nm (see Supporting Information). Protonation of the amine renders the site a poor electron donor and as a result switches off the electron transfer quenching process. The normally very efficient Bodipy-based emission is restored. Similar behaviour has been reported previously for amino-based Bodipy chromophores and their sensing applications.^[22]

Lithium Ion Binding

The small and hard-acid lithium ion is known to predominantly bind to oxygen atoms in ligands such as crown ethers.^[23] We reasoned that the 2,2'-biphenol group can potentially bind to metal ions in a bidentate fashion at low Li^+ concentrations, or may utilise both oxygen atoms in a monodentate coordination mode. The latter case is more likely at high Li^+ concentrations with respect to the ligand. In an initial experiment aliquots of LiClO_4 in dry DMF were added to a solution of **BD** keeping the metal/ligand ($[\text{M}]/[\text{L}]$) ratio below 4. There were no appreciable alterations in recorded absorption spectra for the bands associated with the 2,2'-biphenol unit during the titration. A similar titration performed at $[\text{M}]/[\text{L}]$ ratios greater than 50 dis-

played more distinct modifications to the absorption spectra (Figure 3). The peak at $\lambda_{\text{ABS}} = 320$ nm increased steadily in absorbance to a maximum value; the $[\text{M}]/[\text{L}]$ ratio at this point was ≈ 200 (see Supporting Information). At greater $[\text{M}]/[\text{L}]$ values, a clear new absorption at around 335 nm emerged, and two clear portions were observed in an absorbance vs. $[\text{M}]/[\text{L}]$ plot (Figure 3). Considering the lithium ion concentrations, the region *a* corresponds to the 1:1 complex and region *b* is associated with 2:1 complex formation [Equation (1)] and [Equation (2)]. It can be noted that lithium ion binding may result in deprotonation of the alcohol group(s). Despite the limited data it was possible to apply a binding model to account for complex formation. Application of such a model suggests that $K_1 = 24 \text{ M}^{-1}$ and $K_2 = 3 \text{ M}^{-1}$ (see Supporting Information). Indeed, these values are consistent with previous literature findings.^[24] It is worth noting for this model that the concentration of $\text{Li}^+:\text{BD}$ becomes equal to free **BD** at $[\text{M}]/[\text{L}] = 250$ ($[\text{M}] = 0.035 \text{ M}$). This is roughly the crossing point of *a* and *b*, and the concentration of $(\text{Li}^+)_2:\text{BD}$ is only 5% at this point. The concentration of the 1:1 complex is never higher than 58% (at $[\text{M}] = 0.1 \text{ M}$, $[\text{M}]/[\text{L}] = 700$). In fact, the concentrations for the 1:1 and 1:2 complexes only become equal at $[\text{M}] = 0.3 \text{ M}$ ($[\text{M}]/[\text{L}] = 2000$). Although binding by **BD** towards Li^+ ions is poor, high metal ion concentrations are capable of affecting properties of the dyad.

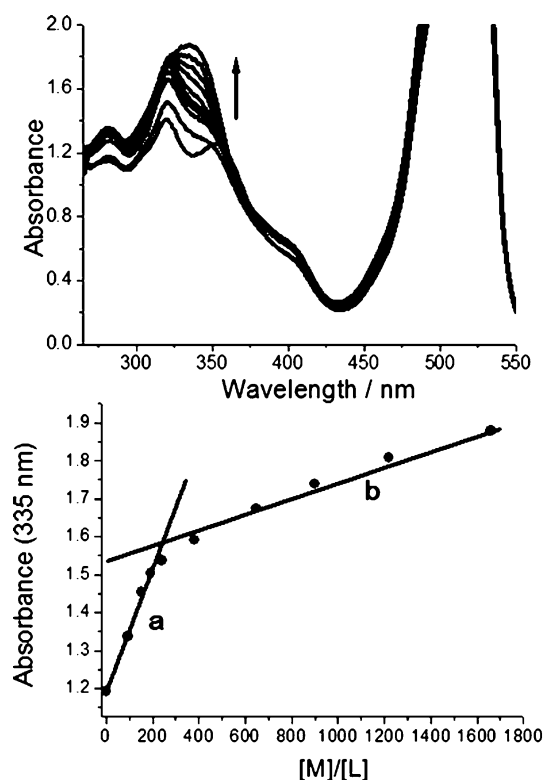


Figure 3. Changes in the absorption spectra recorded for **BD** in dry DMF with addition of LiClO_4 (top). Change in absorbance monitored at 335 nm with respect to the metal/ligand ratio and the two distinct regions to the plot marked *a* and *b*. (bottom). Note: the concentration of **BD** was chosen to optimise absorbance for the short-wavelength absorption bands.



Evidently, the final absorption spectrum is disparate from the starting spectrum and it would appear that metal ion complexation alters the ground-state structure of the 2,2'-biphenol chromophore. It is noted that the absorption spectrum collected by in-situ deprotonation of **BD** using K_2CO_3 in DMF (see Supporting Information) is very similar to that calculated for the 2:1 complex. On the basis of these observations we infer that deprotonation of the alcohol groups in **BD** occurs upon lithium ion binding.

Molecular Modeling

Additional insight into lithium ion binding to **BD** was forthcoming by a series of ground-state molecular structure calculations performed using the Gaussian O3 package.^[25] Several starting geometries were taken and gas-phase structures for **BD** and its adducts were obtained by DFT using the B3LYP parameters and the 6-311G basis set. The structures for lithium adducts (1:1 and 2:1) were calculated as cationic, neutral and anionic species by appropriate deprotonation of the hydroxy group(s). The main reason for this strategy was to acquire some indication of structural changes, and to observe the perturbation in energies for the molecular orbitals. A solvent model was included and additional solvate ligands were added to the lithium ions for the complexes. Purely gas phase structures (see Supporting Information) were deemed less representative of the solute in solution. Clearly, in the coordinating solvent DMF interactions with the phenol groups of the free ligand, or Li^+ ions in the complexes would be expected. Perturbation of the $(\text{Li}^+)_2:\text{BD}$ structure was modelled by placing a single DMF molecule in close proximity to each lithium ion and energy-minimising the calculated gas-phase structure (Figure 4 top). In the first iteration, the semi-empirical PM3 model was used to collect a structure for the solvated adduct. Further refinement was completed by using DFT (B3LYP) and gradually increasing the basis set finally to 6-311G. The computed structure (Figure 4 middle) is interesting in that both lithium ions are displaced away from the aryl rings. Moreover, each lithium ion ends up coordinated to both alcohol units and a DMF solvate; the result is planarization of the 2,2'-biphenol group ($\theta = 44.6^\circ$). An additional DMF solvate^[26] to each lithium ion results in further structural refinements, and structures emerge which are relatively close in energy (see Supporting Information). The lowest energy complex is illustrated in Figure 4 (bottom). One lithium ion is coordinated to two DMF molecules in addition to a phenol group. The other lithium ion is four coordinate and interestingly, a single oxygen acts in a μ_2 -bridging mode (see Supporting Information). The angle $\theta = 51.9^\circ$.

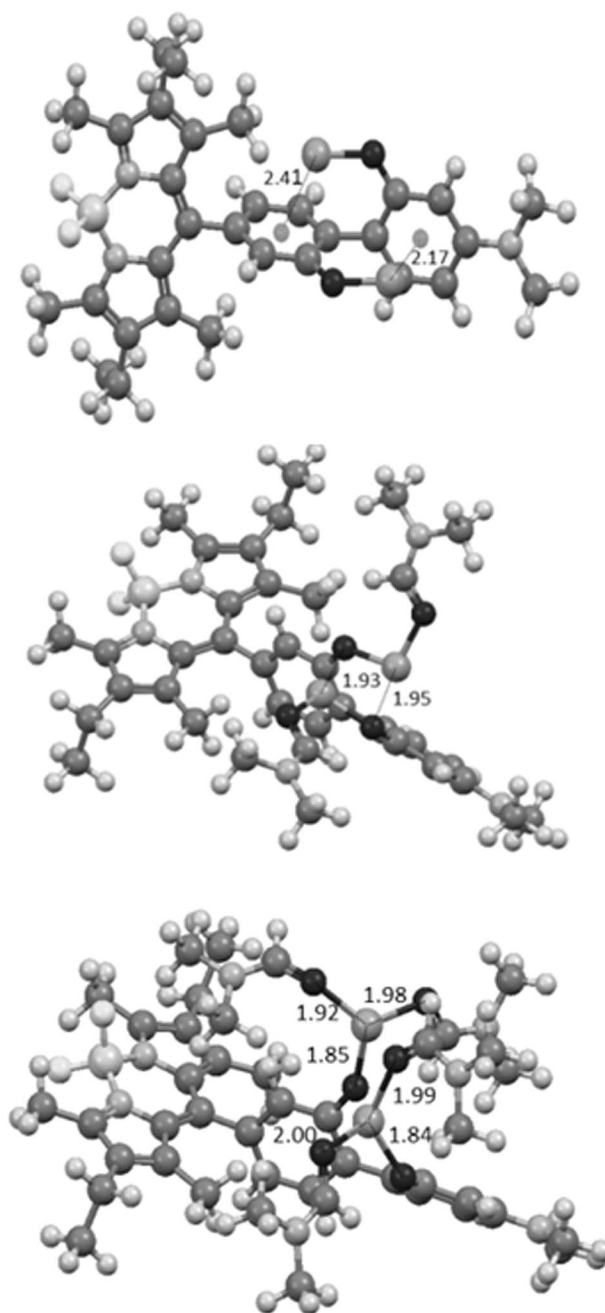


Figure 4. DFT computer calculated energy-minimised gas-phase structures for the di-lithium ion adduct for **BD** (top), bis-DMF solvate (middle) and tetrakis-DMF solvate (bottom) using Gaussian 03 (B3LYP) and a 6-311G basis set. Distances are given in Ångstroms and both alcohol groups are deprotonated to produce the neutral adduct.

A similar perturbation of the $\text{Li}^+:\text{BD}$ structure was accomplished by solvating the lithium ion with two DMF molecules (see Supporting Information). Recalling that two neutral adducts are possible, depending on which phenol group is deprotonated, the values for θ are 50.1° and 51.8° , respectively. Again, application of a DMF solvate model to **BD** had a profound effect on the structure relative to the simple gas-phase model (see Supporting Information); the 2,2'-biphenol group adopts a more planar geometry ($\theta =$

39.2°). It is notable that modelling **BD** with a solvent continuum model (IEFPCM) also resulted in planarization of the 2,2'-biphenol unit ($\theta = 44.8^\circ$). From the model presented here it is inferred that lithium ion binding increases the torsion angle.

Analysis of the molecular orbital diagrams generated for the complexes very much supports the necessity of phenol group deprotonation to generate the neutral adducts (see Supporting Information). In the simple dyad, **BD**, the LUMO is located exclusively on the Bodipy group. The spatial location of the LUMO does not change for the 1:1 lithium adducts, but is lowered significantly in energy (≈ 2 eV) for the mono-cationic form in which both alcohols remained protonated. The perturbation in energy is less severe for the neutral complex, and more reasonable in terms of plausible changes to reduction potentials. The accumulation of positive charge by leaving both alcohol groups protonated for $(\text{Li}^+)_2\text{BD}$ affects both the spatial location of the LUMO and its identity; the molecular orbital is localised on the coordinated 2,2'-biphenol subunit. Upon deprotonation the LUMO is shifted back onto the Bodipy group, and once again, formation of the neutral adduct seems more reasonable in energetic terms. It is noted that the location of the HOMO is highly sensitive to the applied computational method. For example, the HOMO calculated for the gas phase structure of **BD** (DFT, B3LYP, 6-311G) is localized on the Bodipy, and the HOMO-1 is associated with the dimethylaminophenol group. Application of a solvent polarization continuum model, or the DMF solvate model, inverts the two orbitals such that the easiest to oxidise group is the dimethylaminophenol group (see Supporting Information). Certainly these results are more consistent with the electrochemistry findings as discussed later. Again, HOMO energies from calculations for the neutral

species of both the 1:1 and 2:1 complexes are reasonable. It is once again noted that the HOMO is localised on the aminophenol group for the tetrakis DMF solvate lithium complex for **BD** (Figure 5). And the LUMO is associated with the Bodipy group. The HOMO–LUMO energy gap (ΔE) is consistent with electrochemistry findings.

Electrochemistry

The redox chemistry for **BD** was obtained by cyclic voltammetry in dry CH_3CN and using, initially, *N*-tetrabutylammonium perchlorate (0.2 M) as background electrolyte. Considering the wealth of readily available information on the electrochemical behaviour of Bodipy derivatives, the redox response for **BD** was easily interpreted.^[27] The oxidation portion of the cyclic voltammogram displayed a one-electron irreversible wave at $E_1 = +0.73$ V vs. Ag/AgCl corresponding to redox at the dimethylamino site. The irreversibility even at high scan rates is interpreted to represent the breakdown of the nitrogen-based radical cation by deprotonation. A further quasi-reversible oxidation wave was seen at $E_2 = 1.0$ V ($\Delta E = 170$ mV) vs. Ag/AgCl and is associated with electron removal from the Bodipy group. Upon reductive scanning the observed one-electron wave at $E_3 = -1.45$ V ($\Delta E = 80$ mV) is assigned to redox at the Bodipy site. The poor reversibility of the oxidation electrochemistry was not improved by changing the solvent to dry DCM (see Supporting Information). The cyclic voltammetry was repeated using LiClO_4 (0.3 M) as the background electrolyte and a **BD** concentration of 0.5 mM. These conditions are similar to those shown for region *b* in Figure 3. The effect of lithium ion coordination on the redox properties of **BD** was expected to be observed, and there are clear differences in the cyclic voltammogram (see Supporting Information). The oxidative side of the cyclic voltammogram was found to contain three irreversible waves at +0.66 V, +0.88 V and +1.04 V vs. Ag/AgCl. The first wave again is attributed to oxidation of the dimethylamino unit but is more favourable than found in the previous case by around 70 mV. The final wave is taken to be Bodipy-based, meaning that the second wave is based on oxidation of the bridge. Both observations are consistent with deprotonation of **BD** and formation of the neutral lithium ion adduct. Oxidation of both groups is facilitated by delocalisation of negative charge into the aryl ring(s). The one-electron reduction wave for the Bodipy group is shifted to $E_3 = -1.32$ V ($\Delta E = 60$ mV) vs. Ag/AgCl, suggesting that electron density is removed from the group.

Spectroscopy

Interpretation of the excited state deactivation for **BD** in DMF was accomplished using femtosecond up-conversion spectroscopy and ultrafast pump–probe spectroscopy. The fluorescence decay profile collected following a 70 fs laser pulse excitation of **BD** is illustrated in Figure 6. To fit the initial element of the decay profile adequately required the introduction of an ultra-short lifetime ($\tau_1 = 5.5$ ps, $A_1 =$

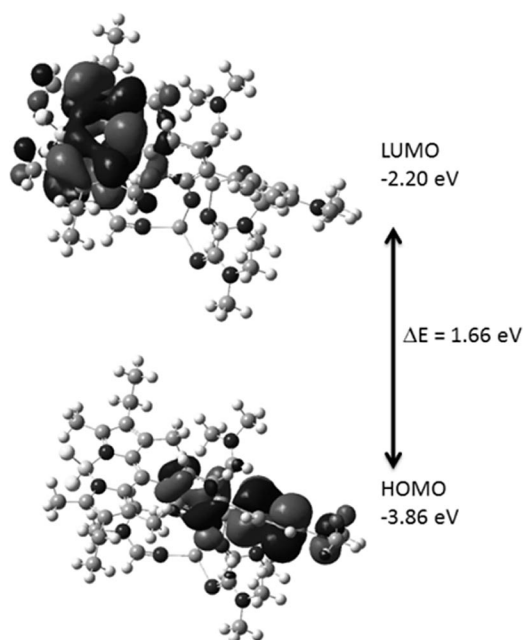


Figure 5. DFT calculated (B3LYP, 6-311G) selected molecular orbitals for the tetrakis DMF solvated di-lithium ion adduct of **BD**.

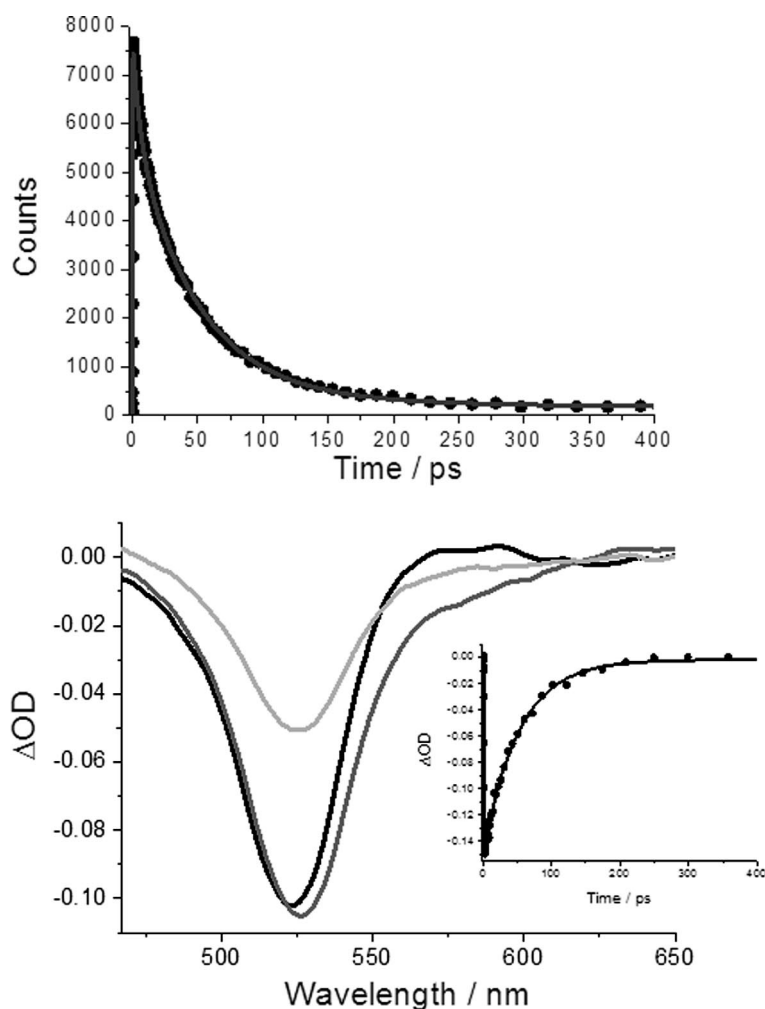


Figure 6. Spectroscopic data collected for **BD** in dry DMF. Top: Fluorescence decay profile as measured by up-conversion spectroscopy and the least-squares fit to the data. Bottom: Selected differential transient absorption spectra at 2 ps (black), 4 ps (grey) and 43 ps (light grey) time delays following excitation at 395 nm with a 70 fs laser pulse. The insert shows the decay monitored at 525 nm and the fit to a single exponential.

23%). The main decay process lifetime $\tau_2 = 48.6$ ps. The fast process is representative of relaxation of the Bodipy S_1 state following its ultrafast generation from the S_2 level, which is preferentially populated at the excitation wavelength. The value of τ_2 is the lifetime of the fully-relaxed S_1 state. Given that the $\phi_{\text{FLU}} = 0.01$ the radiative rate constant ($k_{\text{RAD}} = \phi_{\text{FLU}}/\tau_2$) of $2.0 \times 10^8 \text{ s}^{-1}$ is consistent for a Bodipy derivative.^[28]

Femtosecond pump–probe spectroscopy collected for **BD** in DMF was in full accord with fast deactivation of the Bodipy excited state. Illustrated in Figure 6 are differential transient profiles following laser excitation of **BD** with a 70 fs laser pulse at 395 nm. The hypothesised fast structural alteration is evident by the slight alteration in the bleaching region between 2 to 4 ps. Over some 200 ps the ground state is reformed and there is no evidence in the temporal records for a long-lived species. The two lifetimes obtained by a global fit of the data are 5.2 ps and 52 ps. Both values are remarkably similar to τ_1 and τ_2 , respectively, obtained from up-conversion spectroscopy. Since there is no evidence in

the transient records for a charge transfer state (CTS), it would appear that its formation with a rate constant (k_{CS}) of $\approx 2 \times 10^{10} \text{ s}^{-1}$ is followed by ultrafast charge recombination. Similar behaviour was recently observed for a Bodipy derivative incorporating a naphthalene spacer and is not uncommon.^[29]

In the presence of excess Li^+ ions ($[\text{M}]/[\text{L}] = 2000$) the spectroscopic evidence revealed a change in excited state deactivation kinetics. Remembering that, at this lithium ion concentration, both the 1:1 and 2:1 complexes dominate, the excited state dynamics should be representative of both forms. The first point to note is the significant difference in the decay profile from up-conversion spectroscopy (Figure 7). The initial fast process is enhanced ($\tau_1 = 0.73$ ps, $A_1 = 23\%$), but, importantly, its overall contribution to the decay profile is identical to the free **BD** case. The second contribution lifetime $\tau_2 = 36.9$ ps ($A_2 = 53\%$) and there is a long-lived component $t_3 > 800$ ps ($A_3 = 23\%$). The reason for the final component is not immediately obvious. There is a slight increase in intensity for the steady-state fluores-

cence spectrum of **BD** upon the addition of LiClO_4 (see Supporting Information). However, such a change is probably linked to the alteration in refractive index of the solvent. There is no sign of an additional emission band in the final spectrum. The tail in the up-conversion data is tentatively assigned to low levels of compound degradation due to repetitive laser excitation.

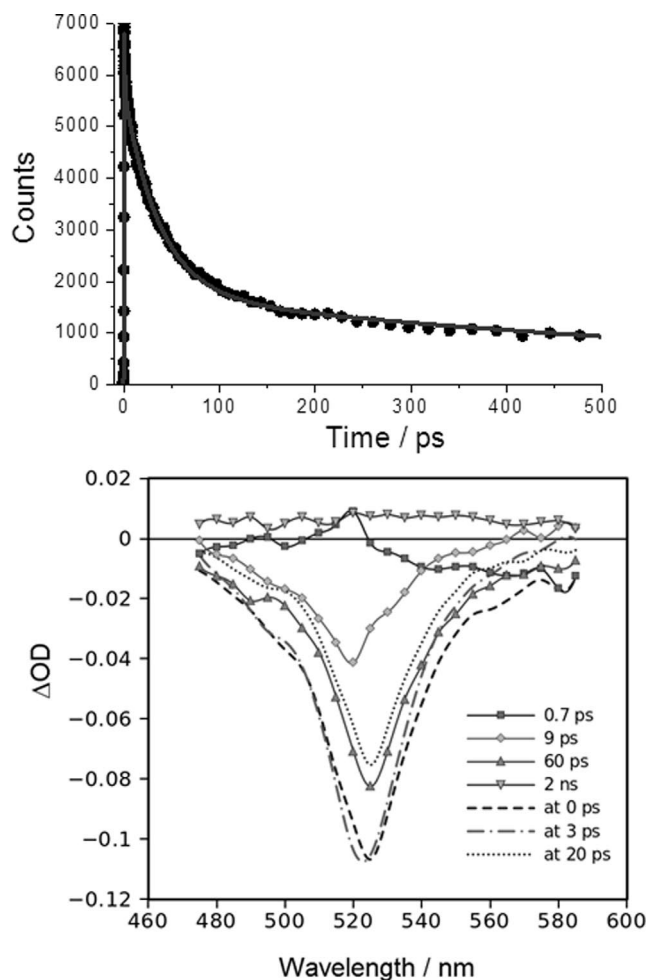


Figure 7. Spectroscopic data collected for **BD** in DMF in the presence of LiClO_4 (excess). Top: Fluorescence decay profile as measured by up-conversion spectroscopy and the least-squares fit to the data. Bottom: Computer generated global fit differential transient absorption spectra following excitation at 395 nm with a 70 fs laser pulse.

In order to fit the transient spectra, a four exponential model was used. This approach gave more than a 10% improvement over a three exponential fit. The absorption decay component spectra for the four exponential model are shown in Figure 7. One point to note is the similarity in spectral shapes for the lithium adducts and **BD** alone, but the dominating component is divided into two lifetimes, 9 ± 5 ps and 60 ± 15 ps. This split is reasonable since one can expect to observe profiles associated with both the 1:1 and 2:1 complexes. The intensity ratio of the 9 ps component to the 60 ps component in absorption is 1:2 and in emission is 1:3, which are reasonably close values. There are two ways to assign the two lifetimes. In the first case the

9 ps and 60 ps components are associated with the 1:1 and 1:2 complexes, respectively. In the context of the two equilibria model discussed above [Equation (1) and Equation (2)] this corresponds to the Li^+ concentration in the sample of approx. 0.6 M ($[\text{M}]/[\text{L}] = 4000$). Alternatively, the 60 ps lifetime is associated with the 1:1 complex ($[\text{Li}^+] = 0.15$ M), and the corollary is that the short lifetime corresponds to the 2:1 complex. For either model one rate for electron transfer is virtually the same as seen for **BD** alone.

Deactivation Model

The basic model for excited-state deactivation of **BD** in DMF in the presence and absence of Li^+ ions is shown in Figure 8. For the ground-state solvated structure of **BD** the two phenol groups of the bridge align at an angle of $\approx 39^\circ$. Under ambient conditions and expressly in solution the two phenol groups will gyrate freely at the connector C–C bond to essentially modulate the angle θ . It is worth noting that unfavourable steric interactions preclude θ reaching zero without distorting significantly the biphenol group. Clearly, there will be an optimum value for θ where the through-bond electronic coupling is high and electron transfer across the bridge is at a maximum. The converse is true for values of θ close to 90° . An angle-independent contribution to through-bond electronic coupling means that an inherent electron transfer process is always present.^[30] Upon formation of the 1:1 and 2:1 complexes the torsion angle θ increases to around 50° suggesting that electronic coupling for both forms is reduced.

Despite the poorly reversible electrochemistry, it is possible to make some tentative estimations for thermodynamic parameters. Using $E_{\text{oo}} = 2.33$ eV, as represented by the mid-point between λ_{EM} and λ_{ABS} , the driving force (ΔG_{CS}) for charge separation in **BD** is ≈ -0.15 eV as calculated using Equation (3).^[31] The terms E_{ox} and E_{red} refer to the potentials for oxidation of the dimethylamino and reduction of the Bodipy groups, respectively.

$$\Delta G_{\text{CS}} = -nF[E_{\text{oo}} - (E_{\text{ox}} - E_{\text{red}})] \quad (3)$$

The driving force ΔG_{CS} is increased to ≈ -0.35 eV upon complex formation. Even considering all the estimations, the alteration in driving force is significant. One problem is the difficulty in assigning unequivocally ΔG_{CS} to either the $\text{Li}^+:\text{BD}$ or $(\text{Li}^+)_2:\text{BD}$ complexes. According to the DFT calculations the HOMO–LUMO gap is the smallest for $(\text{Li}^+)_2:\text{BD}$, which means that ΔG_{CS} will be the greater for the two complexes and thus the 9 ps time constant is assigned to the charge separation in $(\text{Li}^+)_2:\text{BD}$ complex.

Excitation into **BD** populates the S_2 state which deactivates rapidly to the emitting S_1 state in line with Kasha's rule. The fast relaxation event following cross-over from S_2 to S_1 is essentially Bodipy-based. However, there is likely some relaxation contribution from the *meso* appended phenol group since the process is enhanced by interaction of a lithium ion with the alcohol group. As shown, electron transfer from the dimethylamino group to the S_1 state of the

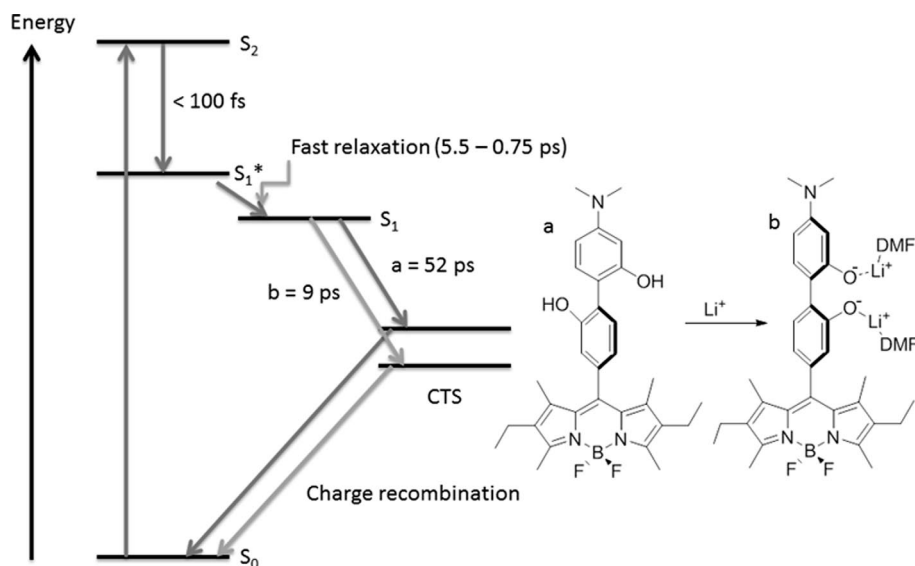


Figure 8. Left: Simple deactivation model for **BD** in DMF showing the processes following excitation into the Bodipy unit.

Bodipy is exergonic, and in free **BD** the CTS is generated in ≈ 52 ps ($k_{\text{CS}} = 1.9 \times 10^{10} \text{ s}^{-1}$). The increase in ΔG_{CS} for $(\text{Li}^+)_2\text{:BD}$ results in a significant proliferation in the rate constant for charge separation to $1.1 \times 10^{11} \text{ s}^{-1}$. It needs to be noted that another factor contributing to the rate of charge separation is the electronic coupling, which depends critically on the dihedral angle θ but cannot be easily evaluated. Considering that charge recombination is too fast to be observed for **BD** alone, the lack of evidence for CTS in the complexed form is not altogether surprising; the electronic π -way is essentially open for both forward and return electron transfer. Such a feature is certainly the downside of the 2,2'-biphenol bridge, and restricts its use as a molecular gate for retarding charge recombination in Bodipy-based systems. The rate of formation of the CTS for $\text{Li}^+:\text{BD}$ is slightly slower than that for **BD** (60 ps vs. 52 ps), which provides one possible explanation for the minor increase in fluorescence intensity at moderate concentrations of Li^+ .

Conclusions

The binding of lithium ions to 2,2'-biphenol is capable of switching the dihedral angle between the two aromatic rings. The dominant feature of lithium ion binding is the perturbation in the energy of the bridge portion. The overall modulation in the electron conduit nature of the 2,2'-biphenol bridge is clearly manifested by the excited state quenching dynamics of the Bodipy chromophore in the dyad **BD**. In fact, as a gate-type unit the 2,2'-biphenol group displays reasonable discrimination (about 6-fold) in forward electron transfer and CTS formation. There is unfortunately no recognizable discrimination in the return electron transfer process. The bridge in the dyad is too good a conduit for electrons, at least in the current molecular system. The practical application of cation binding to manipulate electron flow in bridge systems is clearly limited. Resetting the molecular system quickly is non-trivial, re-

quiring fast competitive binding to pull the metal ion off the assembly. The incorporation of a secondary photo-switch is a more practical way forward. A light-triggered structural alteration could be employed to alter the redox state of the bridge by switching the dihedral angle.^[32]

Experimental Section

Instrumentation: ^1H - and ^{13}C -NMR spectra were recorded with either Bruker AVANCE 300 MHz, JEOL 400 MHz, or JEOL Lambda 500 MHz spectrometers. Chemical shifts for ^1H - and ^{13}C -NMR spectra are referenced relative to the residual protonated solvent. Routine mass spectra were obtained using in-house facilities. Absorption spectra were recorded using a Hitachi U3310 spectrophotometer and corrected fluorescence spectra were recorded using a Hitachi F-4500 spectrometer.

Femto- to pico-second time-resolved absorption spectra were collected using a pump-probe technique described previously.^[33] The femtosecond pulses of a Ti:sapphire generator were amplified by using a multipass amplifier (CDP-Avesta, Moscow, Russia) pumped by a second harmonic of the Nd:YAG Q-switched laser (model LF114, Solar TII, Minsk, Belorussia). The amplified pulses were used to generate second harmonic (400 nm) for sample excitation (pump beam) and the white light continuum for a time-resolved spectrum detection (probe beam). The samples were placed in 1 mm rotating cuvettes, and averaging of 100 pulses at a 10 Hz repetition rate was used to improve the signal-to-noise ratio. The typical response time of the instrument was 150 fs (fwhm). Absorption spectra were recorded prior to and after all experiments to check for compound degradation.

Ultrafast fluorescence decays were measured by an up-conversion method as described previously.^[33] The instrument (FOG100, CDP, Moscow, Russia) utilizes the second harmonic (380 nm) of a 50 fs Ti:sapphire laser (TiF50, CDP, Moscow, Russia) pumped by an Nd laser (Verdi 6, Coherent). The samples were placed in a rotating disk-shaped 1 mm cuvette. A typical resolution for the instrument was 150 fs (fwhm).

Data were collected with the sample in DMF since the solubility of **BD** in MeCN was too low to collect good quality spectra. Time-

resolved transient absorption data were manipulated using the freely available software package, Decfit. In a typical analysis the whole collection of differential absorption spectra was inspected over the full timescale, and decay kinetics were obtained at two specifically chosen wavelengths using an appropriate number of exponentials and instrument response function. Lifetimes obtained by a least-squares fit to the kinetic model were also checked by a global analysis at several different wavelengths. Up-conversion fluorescence lifetimes were obtained by fitting the single-photon-counting data to different kinetic models using a variable Gaussian instrument response function. Analysis was attempted using mono- to tri-exponentials and the stretched exponential function. Best fits were judged by the usual methods of remaining residuals and sigma value.

Binding Studies and Calculations: The concentration of **BD** in dry DMF was optimised to afford an absorption spectrum for which the absorbance in the region $\lambda < 400$ nm was ≈ 1.5 . Weighed known amounts of LiClO₄ were added to the solution which was stirred for 10 min to ensure complete dissolution and equilibration. Collected absorption spectra were analysed globally using the basic theoretical model shown in Supporting Information with the programme Gnumeric.

Computer Calculations: Computational calculations were performed using a 32-bit version of Gaussian03 on a quadruple-core Intel Xeon system with 4GB RAM. The calculations were run in parallel, fully utilising the multi-core processor. To reduce computational time low-level calculations were carried out to minimise structures using Hartree–Fock and a low basis set. Energy-minimised structures were then used to feed high-level DFT calculations initially started with B3LYP and the 3-21G basis set. The complexity of the basis set was increased and results from calculations compared. The 6-311G basis set was deemed sufficient for comparison of structures and for the purpose of mapping HOMO and LUMO energies for molecules. In the specific case of **BD**, a solvent continuum model (IEFPCM) was applied using MeCN as the solvent. Energy minimisation of structures was monitored during calculations using the programme Molden. Standard protocols were used to ascertain completion of structural convergence.

Synthesis: All chemicals were purchased from commercial sources and used as received unless otherwise stated. Basic solvents for synthesis were dried using literature methods. Solvents for spectroscopic investigations were of the highest purity available. All preparations were carried out under N₂ unless otherwise stated. The starting material **1** was prepared according to the literature report.^[18]

Preparation of 2: To the compound 4-iodo-3-hydroxybenzaldehyde **1** (4.00 g, 16.1 mmol) dissolved in dry THF (200 mL) was added triethylamine (9 mL) and pyridine (10 mL). To the mixture was added dropwise diethylcarbonyl chloride (5 mL) and the solution was refluxed overnight. After the reaction mixture was cooled down to room temperature, the white solid formed during reaction was removed by filtration and the filtrate was removed on a rotary evaporator. The resulting residue was dissolved in DCM which was washed with water, separated and dried with MgSO₄. After solvent removal the crude residue was purified by column chromatography (silica gel, DCM/acetone, 100:1) to give the desired product (5.30 g, 15.3 mmol, 95% yield). ¹H NMR (300 MHz, CDCl₃): δ = 9.94 (s, 1 H, CHO), 8.00–7.99 (d, J = 7.8 Hz, 1 H, H³), 7.67–7.66 (d, J = 1.8 Hz, 1 H, H⁶), 7.44–7.41 (dd, J = 7.8 Hz, 1 H, J' = 1.8 Hz, H⁴), 3.59–3.50 (q, J = 6.7 Hz, 2 H, CH₂CH₃), 3.44–3.37 (q, J = 6.7 Hz, 2 H, CH₂CH₃), 1.36–1.31 (t, J = 6.7 Hz, 6 H, 2 × CH₂CH₃) ppm. ¹³C NMR (75 MHz, CDCl₃): δ = 190.5 (CHO), 152.5 (OCON),

139.9, 137.4, 126.8, 123.6, 123.5, 99.5 (6 × Ar-C), 42.3 (CH₂CH₃), 42.0 (CH₂CH₃), 14.3 (CH₃), 13.1 (CH₃) ppm.

Preparation of 3: To a stirred solution of 3-ethyl-2,4-dimethylpyrrole (1.17 mL, 8.6 mmol, 2 equiv.) and compound **2** (1.50 g, 4.3 mmol, 1 equiv.) in DCM (300 mL) was added dropwise trifluoroacetic acid (3 drops). The reaction was allowed to stir at room temperature overnight. DDQ (0.981 g, 4.3 mmol, 1 equiv.) was added in a single portion to the solution and the reaction was left stirring overnight at room temperature. *N,N*-Diisopropylethylamine (9.0 mL, 11 equiv.) and BF₃·Et₂O (9.0 mL, 16 equiv.) were then added, and the reaction was left stirring overnight at room temperature. The reaction mixture was washed six times with water and brine. The separated organic fractions were dried (MgSO₄), filtered and the solvent removed to give a black/dark violet residue with a green tint. The residue was purified by column chromatography (silica gel, DCM) to yield a red solid (1.93 g, 3.1 mmol, 72% yield). ¹H NMR (400 MHz, CDCl₃): δ = 7.92–7.89 (d, J = 7.7 Hz, 1 H, H³), 7.11–7.10 (d, J = 1.8 Hz, 1 H, H⁶), 6.88–6.86 (dd, J = 7.7 Hz, 1 H, J' = 1.8 Hz, H⁴), 3.54–3.49 (q, J = 7.0 Hz, 2 H, NCH₂CH₃), 3.39–3.35 (q, J = 7.0 Hz, 2 H, NCH₂CH₃), 2.50 (s, 6 H, 2 × CH₃), 2.31–2.25 (q, J = 7.4 Hz, 4 H, 2 × CH₂CH₃), 1.40 (s, 6 H, 2 × CH₃), 1.33–1.29 (t, J = 7.0 Hz, 3 H, NCH₂CH₃), 1.22–1.18 (t, J = 7.0 Hz, 3 H, NCH₂CH₃), 0.98–0.95 (t, J = 7.4 Hz, 6 H, 2 × CH₂CH₃) ppm. ¹³C NMR (100 MHz, CDCl₃): δ = 154.2 (OCON), 152.8, 152.7, 139.7, 138.4, 137.4, 137.0, 132.9, 130.4, 126.8, 123.8, 91.3 (11 × Ar-C), 42.3, 42.1, 17.0, 14.6, 14.4, 13.3, 12.5, 12.0 ppm. ¹¹B NMR (128 MHz, CDCl₃): δ = –0.211 (t, J = 32 Hz) ppm. ¹⁹F NMR (376 MHz, CDCl₃): δ = –145.66 (q, J = 32 Hz) ppm.

Preparation of 4: To a solution of 3-(dimethylamino)phenol (10 g, 72.9 mmol) dissolved in THF (280 mL) was added triethylamine (20 mL) and pyridine (10 mL). Diethylcarbonyl chloride (19.0 mL, 207 mmol) was added dropwise over a 10-minute period to the stirred refluxing solution which was continued overnight. The solution was cooled and the white salt formed was removed by filtration and the filtrate was evaporated. The residue was dissolved in DCM which was washed with water, separated and dried with MgSO₄. After removal of the solvent the residue was purified by column chromatography (silica gel, DCM/acetone, 50:1) to give the desired product (16.26 g, 68.8 mmol 94% yield). ¹H NMR (300 MHz, CDCl₃): δ = 7.22–7.16 (t, J = 9 Hz, 1 H, H⁵), 6.57–6.55 (dd, J = 9 Hz, 1 H, J' = 2 Hz, H⁶), 6.48–6.45 (m, 2 H, H² + H⁴), 3.42–3.38 (m, 4 H, 2 × CH₂CH₃), 2.94 (s, 6 H, 2 × NCH₃), 1.25–1.20 (m, 6 H, 2 × CH₂CH₃) ppm. ¹³C NMR (75 MHz, CDCl₃): δ = 154.4 (OCON), 152.6, 151.6, 129.4, 109.6, 109.4, 105.9 (6 × Ar-C), 42.1 (CH₂CH₃), 41.8 (CH₂CH₃), 40.5 (NCH₃), 14.2 (CH₃), 13.4 (CH₃) ppm.

Preparation of 5: To a solution of TMEDA (1.4 mL, 1.1 equiv.) in dry THF (100 mL) at –78 °C was added over 10 minutes a solution of *s*BuLi (1.4 M solution in cyclohexane, 6.7 mL, 1.1 equiv.). The resulting solution was stirred for 15 min at –78 °C and treated with a solution of compound **4** (2.0 g, 8.46 mmol) in dry THF (10 mL) over 30 min. After stirring at –78 °C for 1 h, a solution of iodine (2.47 g, 9.7 mmol) in dry THF (10 mL) was added dropwise over 30 min. The reaction mixture was stirred for 4 h at –78 °C and then overnight at room temperature. After quenching with NH₄Cl (aq) and removal of the organic solvent the residue was extracted with ethyl acetate (100 mL). The crude material after solvent removal was purified by column chromatography (silica gel, DCM/acetone, 50:1) to afford the desired product (2.47 g, 6.8 mmol, 80% yield). ¹H NMR (400 MHz, CDCl₃): δ = 7.53–7.50 (d, J = 9 Hz, 1 H, H³), 6.53–6.52 (d, J = 3 Hz, 1 H, H⁶), 6.36–6.32 (dd, J = 9 Hz,

1 H, $J'=3$ Hz, H^4), 3.55–3.50 (m, 2 H, CH_2CH_3), 3.44–3.39 (m, 2 H, CH_2CH_3), 2.93 (s, 6 H, NCH_3), 1.34–1.29 (t, $J = 7$ Hz, 3 H, CH_2CH_3), 1.25–1.20 (t, $J = 7$ Hz, 3 H, CH_2CH_3) ppm. ^{13}C NMR (100 MHz, CDCl_3): $\delta = 153.2$ (OCON), 152.3, 151.6, 138.5, 111.7, 107.5 ($5 \times \text{Ar-C}$), 73.4 (C-I), 42.2 (CH_2CH_3), 41.9 (CH_2CH_3), 40.3 (NCH_3), 14.3 (CH_3), 13.3 (CH_3) ppm.

Preparation of 6: To a single-necked flask (50 mL) containing **5** (1.3 g, 3.6 mmol) was added pinacolborane (1.1 mL, 7.6 mmol), triethylamine (6.0 mL) and THF (40 mL). The solution was bubbled with dry N_2 , followed by the addition of $\text{PdCl}_2(\text{PPh}_3)_2$ (0.2 g, 0.28 mmol). The reaction mixture was heated and refluxed overnight, then cooled to room temp. and diluted with ethyl acetate (100 mL). The organic layer was washed three times with brine, separated and dried with CaCl_2 . After filtration the solvent was removed and the residue was purified by column chromatography (silica gel, DCM/acetone, 50:1) to give the product (0.843 g, 2.3 mmol, 65% yield). ^1H NMR (400 MHz, CDCl_3): $\delta = 7.61$ – 7.58 (d, $J = 9$ Hz, 1 H, H^3), 6.50–6.47 (dd, $J = 9$ Hz, 1 H, $J'=2$ Hz, H^4), 6.35–6.34 (d, $J = 2$ Hz, 1 H, H^6), 3.51–3.46 (q, $J = 5$ Hz, 2 H, CH_2CH_3), 3.39–3.33 (q, $J = 5$ Hz, 2 H, CH_2CH_3), 2.94 (s, 6 H, $2 \times \text{NCH}_3$), 1.27 (s and m, 12 H + 3 H, $12 \times \text{CH}_3 + \text{CH}_2\text{CH}_3$), 1.19–1.16 (t, $J = 5$ Hz, 3 H, CH_2CH_3) ppm. ^{13}C NMR (100 MHz, CDCl_3): $\delta = 157.9$ (OCON), 154.9, 153.7, 137.1, 108.6, 105.7, 82.7 ($6 \times \text{Ar-C}$), 41.7 (CH_2CH_3), 41.5 (CH_2CH_3), 39.9 (NCH_3), 24.8 (OCC_3), 13.9 (CH_2CH_3), 13.4 (CH_3) ppm (Note: one carbon resonance is missing because of accidental equivalence). ^{11}B NMR (128 MHz, CDCl_3): $\delta = 29.4$ (s) ppm.

Preparation of PBD: To compounds **6** (532 mg, 1.4 mmol) and **3** (913 mg, 1.4 mmol) in DME (50 mL) in a 250 mL two-necked flask was added an aqueous solution of Na_2CO_3 (467 mg in 20 mL of water). The solution was subjected to four freeze-pump-thaw cycles to remove dioxygen. $[\text{Pd}(\text{PPh}_3)_4]$ (170 mg, 0.15 mmol) was then added under nitrogen. After degassing again, the mixture was refluxed overnight and then cooled to room temperature. Water (50 mL) and ethyl acetate (100 mL) were poured into the mixture and the isolated organic layer was dried (MgSO_4), filtered and evaporated under reduced pressure to give the crude product, which was purified by column chromatography [silica gel DCM/acetone (100:1)] to afford the pure product. (196 mg, 0.27 mmol, 19% yield). ^1H NMR (400 MHz, CDCl_3): $\delta = 7.44$ – 7.42 (d, $J = 9$ Hz, 1 H), 7.15–7.09 (m, 3 H), 6.60–6.58 (dd, $J = 9$ Hz, 1 H, $J'=2$ Hz), 6.52–6.51 (d, $J = 2$ Hz, 1 H) ($6 \times \text{Ar-H}$), 3.025–3.18 (m, 8 H, $4 \times \text{NCH}_2\text{CH}_3$), 2.95 (s, 6 H, $2 \times \text{NCH}_3$), 2.25 (s, 6 H, $2 \times \text{CH}_3$), 2.33–2.28 (q, $J = 5$ Hz, 4 H, $2 \times \text{CH}_2\text{CH}_3$), 1.47 (s, 6 H, $2 \times \text{CH}_3$), 1.14–1.08 (q, $J = 5$ Hz, 6 H, $2 \times \text{CH}_2\text{CH}_3$), 1.00–0.96 (m, 12 H, $4 \times \text{NCH}_2\text{CH}_3$) ppm. ^{13}C NMR (100 MHz, CDCl_3): $\delta = 153.9$, 153.7, 153.6, 151.3, 150.1, 149.5, 139.1, 138.6, 135.1, 132.6, 132.4, 132.2, 131.6, 130.7, 41.9, 41.7, 41.6, 41.4, 40.5, 17.0, 14.6, 14.2, 13.7, 13.3, 13.0, 12.4, 11.8 ppm. ^{11}B NMR (128 MHz, CDCl_3): $\delta = -0.153$ (t, $J = 32$ Hz) ppm. ^{19}F NMR (376 MHz, CDCl_3): $\delta = -145.67$ (q, $J = 32$ Hz) ppm.

Preparation of BD: NaOH (3.25 g, 81.3 mmol, 40 equiv.) was added to a solution of **PBD** (1.48 g, 2.0 mmol) in methanol (60 mL) and the mixture was refluxed overnight. After cooling to room temp. water (100 mL) and DCM (100 mL) were poured into the mixture. The separated aqueous layer was neutralized with 1 N HCl and extracted with DCM. The combined organic fractions were washed with water, dried (MgSO_4), filtered and evaporated under reduced pressure to give the crude product which was purified by column chromatography on silica gel with DCM/acetone (1:1) to afford the mono-protected compound (1.26 g, 2.0 mmol). KOH (7.00 g, 125 mmol) was added to a solution of the mono-protected com-

pound (1.26 g, 2.0 mmol) in ethanol (80 mL) and water (8 mL) and the mixture was refluxed for 4 days. To the cooled mixture was added water (100 mL) and DCM (100 mL). The aqueous layer was neutralized with 1 N HCl and extracted with DCM. The combined organic layers were washed with water, separated, dried (MgSO_4) and evaporated under reduced pressure to give the crude product which was purified by column chromatography [silica gel, DCM/acetone (1:1)] to afford **BD** (0.572 g, 1.0 mmol, 54% yield). ^1H NMR (400 MHz, CDCl_3): $\delta = 7.61$ (s, 1 H), 7.43–7.42 (d, $J = 8$ Hz, 1 H), 7.32–7.30 (d, $J = 8$ Hz, 1 H), 6.88–6.86 (d, $J = 8$ Hz, 1 H), 6.58 (s, 1 H), 6.50–6.48 (d, $J = 8$ Hz, 1 H) ($6 \times \text{Ar-H}$), 3.00 (s, 6 H, $2 \times \text{NCH}_3$), 2.63 (s, 2 H, $2 \times \text{OH}$), 2.37 (s, 6 H, $2 \times \text{CH}_3$), 2.29–2.22 (q, $J = 7$ Hz, 4 H, $2 \times \text{CH}_2\text{CH}_3$), 1.47 (s, 6 H, $2 \times \text{CH}_3$), 0.93–0.89 (t, $J = 7$ Hz, 6 H, $2 \times \text{CH}_2\text{CH}_3$) ppm. ^{13}C NMR (100 MHz, CDCl_3): $\delta = 155.0$, 154.1, 153.3, 152.2, 141.0, 137.7, 135.2, 132.5, 132.0, 127.2, 120.5, 117.5, 114.9, 106.4, 102.0, 40.8, 17.3, 14.9, 12.3, 12.1 ppm (Note: two carbon resonances are missing because of accidental equivalence). ^{11}B NMR (128 MHz, CDCl_3): $\delta = 1.69$ (br) ppm. ES-MS *m/z* fnd 515.4 calcd. $[\text{M} - \text{OH}]^+$ 515.4.

Supporting Information (see footnote on the first page of this article): Copies of ^1H NMR and ^{13}C NMR spectra for **BD** and **PBD**, binding model and data, additional figures molecular modeling pictures and CV data.

Acknowledgments

The authors thank the Engineering and Physical Sciences Research Council (EPSRC) (EP/G04094X/1) for financial support. Mass spectrometry data were acquired at the EPSRC UK National Mass Spectrometry Facility at Swansea.

- [1] a) J. Lin, I. A. Balabin, D. N. Beratan, *Science* **2005**, *310*, 1311–1313; b) J. N. Onuchi, D. N. Beratan, J. R. Winkler, H. B. Gray, *Annu. Rev. Biophys. Biomol. Struct.* **1992**, *21*, 349–77.
- [2] G. S. Singhal, G. Renger, S. K. Sopory, K. D. Irrgang, Govindjee (Eds.), *Concepts in Photobiology: Photosynthesis and Photomorphogenesis*, Springer, Dordrecht, **1999**.
- [3] M. A. Steffen, K. Lao, S. G. Boxer, *Science* **1994**, *264*, 810–816.
- [4] J. L. Dempsey, J. R. Winkler, H. B. Gray, *Chem. Rev.* **2010**, *110*, 7024–7039.
- [5] L. F. Agnati, M. Zoli, I. Strömberg, K. Fuxe, *Neuroscience* **1995**, *69*, 711–726.
- [6] R. I. Cukier, D. G. Nocera, *Ann. Rev. Phys. Chem.* **1998**, *49*, 337–369.
- [7] P. Faller, A. Pascal, A. W. Rutherford, *Biochemistry* **2001**, *40*, 6431–6440.
- [8] N. J. Fraser, H. Hashimoto, R. J. Cogdell, *Photosynth. Res.* **2001**, *70*, 249–256.
- [9] a) M. R. Wasielewski, *Chem. Rev.* **1992**, *92*, 435–461; b) M. D. Ward, *Chem. Soc. Rev.* **1997**, *26*, 365–375.
- [10] a) F. D'Souza, A. N. Amin, M. E. El-Khouly, N. K. Subbaiyan, M. E. Zandler, S. Fukuzumi, *J. Am. Chem. Soc.* **2012**, *134*, 654–664; b) A. Marcos Ramos, S. C. J. Meskers, E. H. A. Beckers, R. B. Prince, L. Brunsveld, R. A. J. Janssen, *J. Am. Chem. Soc.* **2004**, *126*, 9630–9644; c) S. D. Straight, J. Andréasson, G. Kodis, A. L. Moore, T. A. Moore, D. Gust, *J. Am. Chem. Soc.* **2005**, *127*, 2717–2724; d) P. P. Lainé, F. Bedioui, F. Loiseau, C. Chiorboli, S. Campagna, *J. Am. Chem. Soc.* **2006**, *128*, 7510–7521.
- [11] M. T. Colvin, A. Butler Ricks, M. R. Wasielewski, *J. Phys. Chem. A* **2012**, *116*, 2184–2191.
- [12] a) J. Seth, V. Palaniappan, R. W. Wagner, T. E. Johnson, J. S. Lindsey, D. F. Bocian, *J. Am. Chem. Soc.* **1996**, *118*, 11194–11207; b) A. C. Benniston, A. Harriman, P. Li, P. V. Patel, C. A. Sams, *Chem. Phys. Phys. Chem.* **2005**, *7*, 3677–3679; c)

- A. C. Benniston, A. Harriman, P. Li, P. V. Patel, C. A. Sams, *Chem. Eur. J.* **2008**, *14*, 1710–1717.
- [13] a) A. Osuka, J.-Y. Shin, R. Yoneshima, H. Shiratori, T. Ohno, K. Nozaki, Y. Nishimura, I. Yamazaki, S. Taniguchi, T. Shimizu, T. Okada, *J. Porphyrins Phthalocyanines* **1999**, *3*, 729–741; A. C. Benniston, A. Harriman, P. Li, C. A. Sams, M. D. Ward, *J. Am. Chem. Soc.* **2004**, *126*, 13630–13633.
- [14] a) L. Venkataraman, J. E. Klare, C. Nuckolls, M. S. Hybertsen, M. L. Steigerwald, *Nature* **2006**, *442*, 904–907; b) L. Cui, B. Liu, D. Vonlanthen, M. Mayor, Y. Fu, J.-F. Li, T. Wandlowski, *J. Am. Chem. Soc.* **2011**, *133*, 7332–7335; c) D. Hanss, O. S. Wenger, *Eur. J. Inorg. Chem.* **2009**, 3778–3790; d) D. Vonlanthen, A. Mishchenko, M. Elbing, M. Neuburger, T. Wandlowski, M. Mayor, *Angew. Chem.* **2009**, *121*, 9048; *Angew. Chem. Int. Ed.* **2009**, *48*, 8886–8890.
- [15] a) J. S. Park, E. Karnas, K. Ohkubo, P. Chen, K. M. Kadish, S. Fukuzumi, C. W. Bielawski, T. W. Hudnall, V. M. Lynch, J. L. Sessler, *Science* **2010**, *329*, 1324–1326; b) F. D'Souza, N. K. Subbairan, Y. Xie, J. P. Hill, K. Ohkubo, S. Fukuzumi, *J. Am. Chem. Soc.* **2009**, *131*, 16138–16146.
- [16] a) M. Maus, W. Rettig, D. Bonafoux, R. Lapouyade, *J. Phys. Chem. A* **1999**, *103*, 3388–3401; b) M. W. Holman, P. Yan, K.-C. Ching, R. Liu, F. I. Ishak, D. M. Adams, *Chem. Phys. Lett.* **2005**, *413*, 501–505; c) A. C. Benniston, A. Harriman, P. Li, P. V. Patel, J. P. Rostron, C. A. Sams, *J. Phys. Chem. A* **2006**, *110*, 9880–9886.
- [17] F. A. Cotton, G. Wilkinson, *Advanced Inorganic Chemistry A Comprehensive Text*, Fourth Edition, John Wiley & Sons, **1980**.
- [18] A. T. Shinde, S. B. Zangade, S. B. Chavan, A. Y. Vibhute, Y. S. Nalwar, Y. B. Vibhute, *Synth. Commun.* **2010**, *40*, 3506–3513.
- [19] a) A. Loudet, K. Burgess, *Chem. Rev.* **2007**, *107*, 4891–4932; b) T. E. Wood, A. Thompson, *Chem. Rev.* **2007**, *107*, 1831–1861; c) N. Boens, V. Leen, W. Dehaen, *Chem. Soc. Rev.* **2012**, *41*, 1130–1172.
- [20] J. E. Barbarini, R. Rittner, N. F. Höehr, J. Suwinski, *Biorg. Chem.* **1997**, *25*, 37–41.
- [21] G. J. Hedley, A. Ruseckas, A. Harriman, I. D. W. Samuel, *Angew. Chem.* **2011**, *123*, 6764–6767; *Angew. Chem. Int. Ed.* **2011**, *50*, 6634–6637.
- [22] a) M. Kollmannsberger, K. Rurack, U. Resch-Genger, J. Daub, *J. Phys. Chem. A* **1998**, *102*, 10211–10220; b) W. Qin, M. Baruah, W. M. De Borggraeve, N. Boens, *J. Photochem. Photobiol. A: Chem.* **2006**, *183*, 190–197; c) M. Baruah, W. Qin, N. Basarić, W. M. De Borggraeve, N. Boens, *J. Org. Chem.* **2005**, *70*, 4152–4157.
- [23] U. Olsher, R. M. Izatt, J. S. Bradshaw, N. K. Dalley, *Chem. Rev.* **1991**, *91*, 137–164.
- [24] a) M. C. Masiker, C. L. Mayne, B. J. Boone, A. M. Orendt, E. M. Eyring, *Magn. Reson. Chem.* **2010**, *48*, 94–100; b) A. C. Benniston, A. Harriman, P. V. Patel, C. A. Sams, *Eur. J. Org. Chem.* **2005**, 4680–4686.
- [25] M. J. Frisch, G. W. Trucks, H. B. Schlegel, G. E. Scuseria, M. A. Robb, J. R. Cheeseman, J. A. Montgomery Jr., T. Vreven, K. N. Kudin, J. C. Burant, J. M. Millam, S. S. Iyengar, J. Tomasi, V. Barone, B. Mennucci, M. Cossi, G. Scalmani, N. Rega, G. A. Petersson, H. Nakatsuji, M. Hada, M. Ehara, K. Toyota, R. Fukuda, J. Hasegawa, M. Ishida, T. Nakajima, Y. Honda, O. Kitao, H. Nakai, M. Klene, X. Li, J. E. Knox, H. P. Hratchian, J. B. Cross, V. Bakken, C. Adamo, J. Jaramillo, R. Gomperts, R. E. Stratmann, O. Yazyev, A. J. Austin, R. Cammi, C. Pomelli, J. W. Ochterski, P. Y. Ayala, K. Morokuma, G. A. Voth, P. Salvador, J. J. Dannenberg, V. G. Zakrzewski, S. Dapprich, A. D. Daniels, M. C. Strain, O. Farkas, D. K. Malick, A. D. Rabuck, K. Raghavachari, J. B. Foresman, J. V. Ortiz, Q. Cui, A. G. Baboul, S. Clifford, J. Cioslowski, B. B. Stefanov, G. Liu, A. Liashenko, P. Piskorz, I. Komaromi, R. L. Martin, D. J. Fox, T. Keith, M. A. Al-Laham, C. Y. Peng, A. Nanayakkara, M. Challacombe, P. M. W. Gill, B. Johnson, W. Chen, M. W. Wong, C. Gonzalez, J. A. Pople, *Gaussian 03*, Gaussian, Inc., Wallingford CT, **2004**.
- [26] The limiting coordination number of four was chosen on the basis of the X-ray structure for bis[(*N,N*-dimethylformamide)pyrocatecholato-*O,O'*]lithium as a model, see: C. Näther, A. John, K. Ruppert, H. Bock, *Acta Crystallogr., Sect. C* **1996**, *52*, 1166–1168.
- [27] R. Y. Yai, A. J. Bard, *J. Phys. Chem. B* **2003**, *107*, 5036–5042.
- [28] a) R. Ziessel, G. Ulrich, A. Harriman, *New J. Chem.* **2007**, *31*, 496–501; b) W. Qin, M. Baruah, M. Van der Auweraer, F. C. De Schryver, N. Boens, *J. Phys. Chem. A* **2005**, *109*, 7371–7384; c) M. Baruah, W. Qin, C. Flors, J. Hofkens, R. A. L. Vallée, D. Beljonne, M. Van der Auweraer, W. M. De Borggraeve, N. Boens, *J. Phys. Chem. A* **2006**, *110*, 5998–6009; d) W. Qin, T. Rohand, W. Dehaen, J. N. Clifford, K. Driesen, D. Beljonne, B. Van Averbeke, M. Van der Auweraer, N. Boens, *J. Phys. Chem. A* **2007**, *111*, 8588–8597; e) W. Qin, M. Baruah, M. Sliwa, M. Van der Auweraer, W. M. De Borggraeve, D. Beljonne, B. Van Averbeke, N. Boens, *J. Phys. Chem. A* **2008**, *112*, 6104–6114; f) N. Boens, V. Leen, W. Dehaen, L. Wang, K. Robeyns, W. Qin, X. Tang, D. Beljonne, C. Tonnelé, J. M. Pardes, M. J. Ruedas-Rama, A. Orte, L. Crovetto, E. M. Talavera, J. M. Alvarez-Pez, *J. Phys. Chem. A* **2012**, *116*, 9621–9531.
- [29] A. C. Benniston, S. Clift, J. Hagon, H. Lemmetyinen, N. V. Tkachenko, W. Clegg, R. W. Harrington, *ChemPhysChem* **2012**, *13*, 3672–3681.
- [30] a) R. M. Williams, *Photochem. Photobiol. Sci.* **2010**, *9*, 1018–1026; b) A. C. Benniston, A. Harriman, *Chem. Soc. Rev.* **2006**, *35*, 169–179.
- [31] D. Rehm, A. Weller, *Isr. J. Chem.* **1970**, *8*, 259–271.
- [32] a) S. M. Parker, M. A. Ratner, T. Seideman, *J. Chem. Phys.* **2011**, *135*, 224301–6; b) A. C. Benniston, A. Harriman, S. J. Yang, R. W. Harrington, *Tetrahedron Lett.* **2011**, *52*, 5315–5318.
- [33] N. V. Tkachenko, L. Rantala, A. Y. Tuaber, J. Helaja, P. H. Hynninen, H. Lemmetyinen, *J. Am. Chem. Soc.* **1999**, *121*, 9378–9387.

Received: June 13, 2013

Published Online: September 4, 2013